Vinculin regulates cell-surface E-cadherin expression by binding to β-catenin

Xiao Peng, Laura E. Cuff, Cort D. Lawton and Kris A. DeMali*

Department of Biochemistry, University of Iowa Roy J. Carver College of Medicine, Iowa City, IA 52242, USA

*Author for correspondence (kris-demali@uiowa.edu)

Accepted 23 November 2009
Journal of Cell Science 123, 567-577

doi:10.1242/jcs.056432

Summary

Vinculin was identified as a component of adherens junctions 30 years ago, yet its function there remains elusive. Deletion studies are consistent with the idea that vinculin is important for the organization of cell-cell junctions. However, this approach removes vinculin from both cell-matrix and cell-cell adhesions, making it impossible to distinguish its contribution at each site. To define the role of vinculin in cell-cell junctions, we established a powerful short hairpin-RNA-based knockdown/substitution model system that perturbs vinculin preferentially at sites of cell-cell adhesion. When this system was applied to epithelial cells, cell morphology was altered, and cadherin-dependent adhesion was reduced. These defects resulted from impaired E-cadherin cell-surface expression. We have investigated the mechanism for the effects of vinculin and found that the reduced surface E-cadherin expression could be rescued by introduction of vinculin, but not of a vinculin A50I substitution mutant that is defective for β-catenin binding. These findings suggest that an interaction between β-catenin and vinculin is crucial for stabilizing E-cadherin at the cell surface. This was confirmed by analyzing a β-catenin mutant that fails to bind vinculin. Thus, our study identifies vinculin as a novel regulator of E-cadherin function and provides important new insight into the dynamic regulation of adherens junctions.

Key words: Adherens junctions, β-catenin, Cadherin, Cell-cell junctions, Vinculin

Introduction

The formation of adhesive structures between adjacent cells, including adherens and tight junctions, contributes to the establishment of cell polarity, differentiation and survival. Cadherins are one of the major constituents of adherens junctions and play important roles in the formation and maintenance of contacts between cells during development (Gumbiner, 1996; Takeichi, 1994; Tepass et al., 2000). Although many cytoplasmic binding partners for the cadherins have been identified, it will be essential to gain additional insight into how these molecules govern cadherin function to fully understand how cell-cell adhesions assemble during normal biological processes and how they become deregulated in diseased states.

In order to mediate cell-cell adhesion, newly synthesized cadherins must be packaged in the Golgi and transported to the cell surface, where they either engage in productive adhesive interactions or are internalized into early or sorting endosomes (reviewed by Bryant and Stow, 2004; Yap et al., 2007). From this point, cadherins are recycled back to the plasma membrane or are transported to the late endosomes and subsequently degraded in lysosomes. Proteins that bind to the cadherin cytoplasmic domain play crucial roles in E-cadherin trafficking. p120-catenin, for example, prevents cadherin turnover (Davis et al., 2003; Ireton et al., 2002; Xiao et al., 2003) and if p120-catenin is not directly recruited to the membrane, most cadherins are internalized and often degraded (Davis et al., 2003; Xiao et al., 2003). By contrast, β-catenin is required to facilitate cadherin transport to the plasma membrane. Mutant forms of E-cadherin that do not bind β-catenin are either delayed in their arrival at the plasma membrane or fail to localize to the junctions (Chen et al., 1999; Miranda et al., 2001). Taken together, these observations have led to the idea that many of the proteins recruited to the cadherin cytoplasmic domain regulate cadherin availability at the cell surface.

Vinculin, a well-known component of cell-matrix adhesions, is also present at the cytoplasmic domains of cadherins (Burridge and Feramisco, 1980; Geiger, 1979; Geiger et al., 1981). It binds α- and/or β-catenin, which also bind to one another (Hazan et al., 1997; Watabe-Uchida et al., 1998; Barth et al., 1997). Vinculin exists in at least two conformations. When in the closed, 'inactive' conformation, extensive interactions between the head and tail domains prevent detectable binding to most of its ligands (Johnson and Craig, 1995; Bakolitsa et al., 2004). The protein takes on an 'active' conformation after cooperative and simultaneous binding of two different ligands. This activation involves displacement of the head-tail interactions and leads to a significant accumulation of ternary complexes (Chen et al., 2006; Cohen et al., 2005). Active vinculin then binds a number of proteins that have both signaling and structural roles that are essential for cell adhesion (reviewed in Ziegler et al., 2006).

Most of the attention on vinculin has focused on its presence in cell-matrix adhesions, leaving a gap in our knowledge of its function in cell-cell junctions. Nevertheless, some data on the role of vinculin at the latter site has emerged and provides evidence for the notion that vinculin modulates adhesion at sites of cell-cell contact. First, Hazan and colleagues showed that in cells lacking α-catenin, vinculin is required for cadherin-based cell adhesion complexes through the direct interaction with β-catenin (Hazan et al., 1997). Second, mice null for vinculin die during embryonic development (Xu et al., 1998a). Death results from severe developmental abnormalities in the heart and from brain defects that are consequences of a failure in neural tube closure (Xu et al., 1998a). Third, mice in which vinculin has been disrupted specifically in cardiac myocytes experience sudden death due to abnormal adherens junctions that lead to disruption of the intercalated disc structure in cardiac muscle (Zemljic-Harpf et al., 2007; Zemljic-Harpf et al., 2004). Finally, studies in tumor cells

Journal of Cell Science

have indicated that cell-cell adhesion is lost during the initial stages of tumor formation at a time when vinculin becomes mislocalized (Kawahara et al., 1999; Lifschitz-Mercer et al., 1997; Meyer and Brinck, 1997; Sadano et al., 1992; Somiari et al., 2003). Although all of the phenotypes identified in these studies involve improper cell-cell adhesion, and thus suggest that vinculin is required for adhesion, in each of the settings, vinculin function at cell-matrix adhesions is also perturbed. Thus, it is impossible to draw definitive conclusions about the contribution of adherens junction-resident vinculin to the observed phenotype. Adding controversy to the role of vinculin in adherens junctions is the fact that vinculin overexpression studies are uninformative; the overexpressed protein neither integrates readily into pre-existing cell-cell adhesions nor turns over in a manner that is consistent with cadherin-catenin dynamics (Yamada et al., 2005).

In the study described here, we used a new approach to test the role that vinculin plays at cell-cell adhesions. Specifically, we generated a powerful vinculin shRNA knockdown/substitution model system that preferentially depletes vinculin from adherens junctions while leaving its expression at cell-matrix adhesions intact. We have used this model system to explore the mechanism whereby vinculin regulates adherens junctions and found that the absence of vinculin leads to impaired epithelial cell-cell adhesion due to a decrease in cell-surface expression of E-cadherin, without a change in total E-cadherin. We also show that the ability of vinculin to regulate E-cadherin availability at the plasma membrane requires its interaction with β-catenin and is blocked by a β-catenin mutant that fails to bind vinculin.

Results

The affinity of vinculin for cell-matrix adhesions is much higher than its affinity for cell-cell adhesions (Bakolitsa et al., 2004), and only a small amount of vinculin is required to maintain cell-matrix adhesion (Xu et al., 1998a; Xu et al., 1998b). Thus, it seemed plausible that the function of vinculin in cell-cell adhesions could be disturbed while leaving its cell-matrix adhesions function intact. We tested this possibility by using small hairpin RNAs (shRNAs) to inhibit vinculin expression in human mammary epithelial cells (MCF10a cell line). Analysis of stably infected cells expressing the shRNAs (knockdown cells, KD) showed that we could suppress vinculin levels by 80-90% compared to the cells infected with control vector (Cont) (Fig. 1A). Expression of an shRNA containing a scramble of this sequence produced no change in vinculin levels (supplementary material Fig. S1).

To potentially rescue the expected cell-cell adhesion defects due to vinculin inhibition, it was necessary to also generate wild-type and mutant versions of vinculin to reintroduce into our cell lines. To make them resistant to the shRNAs used to target the endogenous human vinculin, we used the chick vinculin (cVIN) sequence. Human and chick vinculins are functionally interchangeable (>95% sequence identity), and the vast majority of the published studies involving vinculin overexpression have employed the chick protein. Fig. 1A showed that GFP-tagged chick vinculin (KD/GFP-cVIN) could be successfully expressed in cells also expressing the shRNAs directed against human vinculin. This approach resulted in a 36% increase in vinculin levels compared to the control cells (Fig. 1A). Similarly, by using sequential infection, stable cell lines expressing GFP and shRNAs against vinculin (KD/GFP) were established to analyze the role of vinculin in adherens junctions in the absence of a rescue construct. As a control, we also established stable cells expressing GFP and the vector without shRNAs sequence (Cont/GFP) (Fig. 1A).

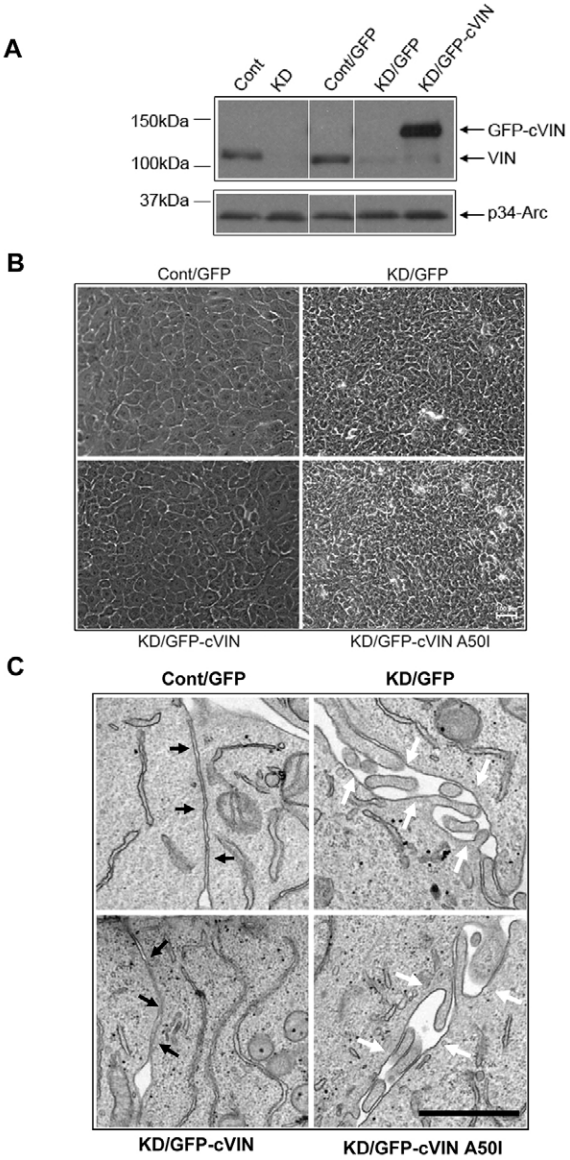

Fig. 1. Stable inhibition of vinculin in breast epithelial cells by RNA interference. (**A**) MCF10a cells were infected with GFP, GFP-tagged chick vinculin (GFP-cVIN) or a mutant version of vinculin (GFP-cVIN A50I), and then infected a second time with either an empty vector (Cont) or a vector encoding a shRNA targeting human vinculin (KD). Lysates were harvested from cell lines stably expressing these plasmids, and western blot analysis was performed using antibodies against vinculin (VIN) or the p34-Arc subunit of the Arp2/3 complex as a loading control. All of the samples were prepared and analyzed in the same experiment; the white line indicates where the western blot was cut to remove some irrelevant samples. (**B**) Phase-contrast images of MCF10a cells stably expressing the indicated constructs. Scale bar: 100 μm. (**C**) Transmission EM micrographs of MCF10a cells stably expressing the indicated constructs. Scale bar: 1 μm. The black arrows indicate adherens junctions; the white arrows indicate regions between cells where adherens junctions are disrupted.

Vinculin inhibition alters E-cadherin-mediated cell-cell adhesion

Phase-contrast images of cells harboring the shRNAs against vinculin (KD/GFP) showed that in the absence of vinculin, epithelial cell morphology was altered, and the honeycomb shape that is

characteristic of epithelial cells was lost (Fig. 1B). These morphological changes could be rescued by expression of cVIN (Fig. 1B), suggesting this effect is specifically due to loss of vinculin and not due to off-target silencing. Furthermore, these effects were not due to differences in growth rates (supplementary material Fig. S2) and they were not limited to MCF10a cells because another epithelial cell line (Caco-2) exhibited similar morphological changes when vinculin expression was inhibited (supplementary material Fig. S3).

To determine whether the phenotypic changes in the vinculin knockdown cells were the result of a loss of adherens junctions, we examined the morphology of the cells using transmission EM. Using this approach, the control (Cont/GFP) and wild-type rescued cells (KD/GFP-cVIN) formed adherens junctions in the regions between neighboring cells. By contrast, the knockdown cells appeared to be extending protrusions to make contact with adjacent cells, but in many instances failed to do so (Fig. 1C).

To test whether these morphological changes were due to a preferential depletion of vinculin from sites of cell-cell adhesion, we examined colocalization of vinculin with paxillin in focal adhesions or with β-catenin in adherens junctions. In the Cont/GFP cells, vinculin colocalized with both markers. By contrast, in the knockdown cells the residual vinculin localized to focal adhesions but not adherens junctions (Fig. 2A). In addition, β-catenin staining revealed that the adherens junctions were disrupted in the knockdown cells. We quantified the amount of the residual vinculin that was present in focal adhesions or in adherens junctions in the knockdown cells and found that there is a 81% loss of vinculin from adherens junctions but only an insignificant loss from focal adhesions (Fig. 2B). In further support of a preferential depletion of vinculin from adherens junctions, we found that E-cadherin failed to co-precipitate with GFP recovered from the knockdown cells but readily bound to GFP-vinculin in the wild-type rescued cells (Fig. 2C, compare KD/GFP and KD/GFP-WT cVin).

To assess the contribution, if any, that changes in cell-matrix adhesion have on the observed morphological differences, we examined adhesion to the extracellular matrix ligands, fibronectin and collagen (Fig. 3A,B). We consistently found only a modest, and statistically insignificant, decrease in adhesion. This effect was not limited to cells plated on a saturating dose of fibronectin or collagen because the knockdown cells were able to adhere to sub-saturating concentrations of fibronectin to the same extent as the control cells (Fig. 3C). Also, we did not see changes in cell morphology when cells were plated at low density (supplementary material Fig. S4). The lack of an effect on cell-matrix adhesion might be a consequence of the facts that we (Fig. 2 and supplementary material Fig. S5) and others (Harborth et al., 2001; Moese et al., 2007) have not been able to completely deplete vinculin from cell-matrix adhesions by RNA interference, and that only a small amount of vinculin is needed to support cell-matrix adhesion (Xu et al., 1998a; Xu et al., 1998b).

To determine whether the morphological differences that we observed in the vinculin knockdown cells were due to a loss of cadherin-mediated adhesion, we measured the ability of the cells to bind to the extracellular domains of cadherin proteins. This assay examines homophilic ligation of cadherin at points of cell adhesion to substrata coated with recombinant cadherin ligands. Unlike the control cells, which adhered to and spread well on the cadherin extracellular domains, the vinculin knockdown cells were significantly impaired in adhesion (Fig. 4). These defects were rescued when cVIN was expressed in the knockdown cells (Fig. 4). As a negative control, cVIN rescued cells were pre-incubated with the E-cadherin function-blocking antibody DECMA, which results in very few cells adhering, indicating that the adhesion is mediated by E-cadherin (Fig. 4). Taken together, these findings suggest that the altered morphology in the vinculin knockdown cells results from impaired cell-cell adhesion but not impaired cell-matrix adhesion.

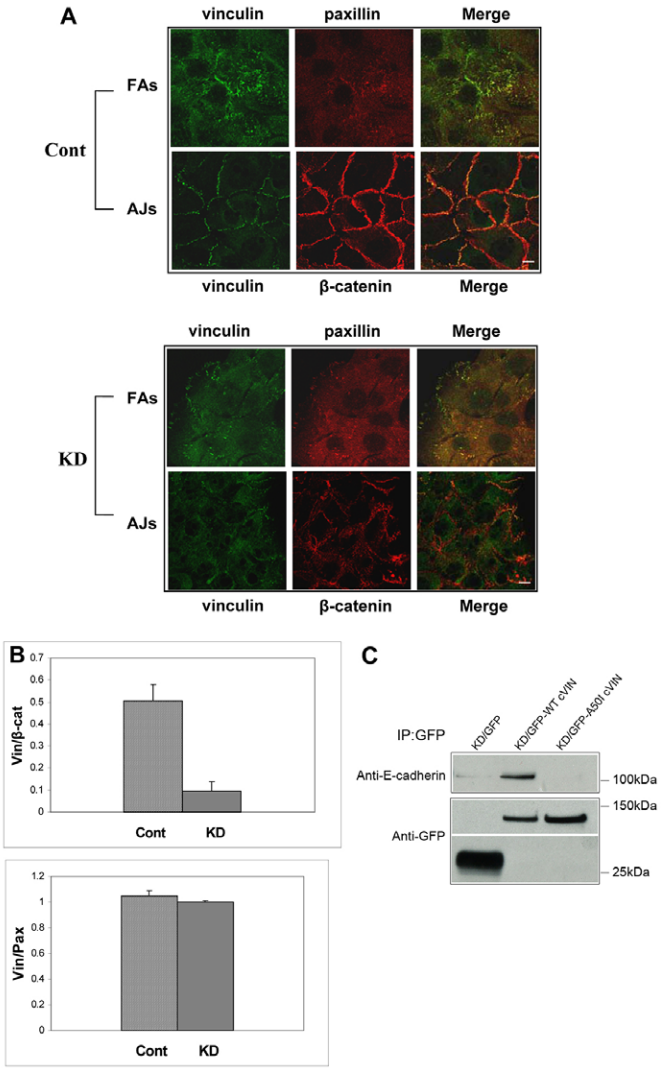

Fig. 2. Inhibition of vinculin preferentially depleted vinculin from cell-cell adhesion but not cell-matrix adhesions. (**A**) MCF10a cells stably expressing the indicated constructs were stained with antibodies against the adherens junction (AJ) marker β-catenin or the focal adhesion (FA) marker (paxillin). Using confocal microscopy different focal planes were isolated and photographed. Scale bar: 10 µm. (**B**) Ratiometric analysis of vinculin, β-catenin (β-cat) and paxillin (Pax) fluorescence intensity at adherens junctions or focal adhesions. Fluorescence intensity of vinculin staining was expressed as a ratio of β-catenin or paxillin fluorescence intensity at the same individual cell–cell contacts. Data are means ± s.e.m. (n=30 and are representative of three independent experiments). (**C**) GFP, wild-type GFP-cVIN or GFP-cVIN A50I were immunoprecipitated, washed, fractionated by SDS-PAGE, and immunoblotted with an antibody against E-cadherin. The blot was stripped and re-probed for the precipitated levels of each GFP protein.

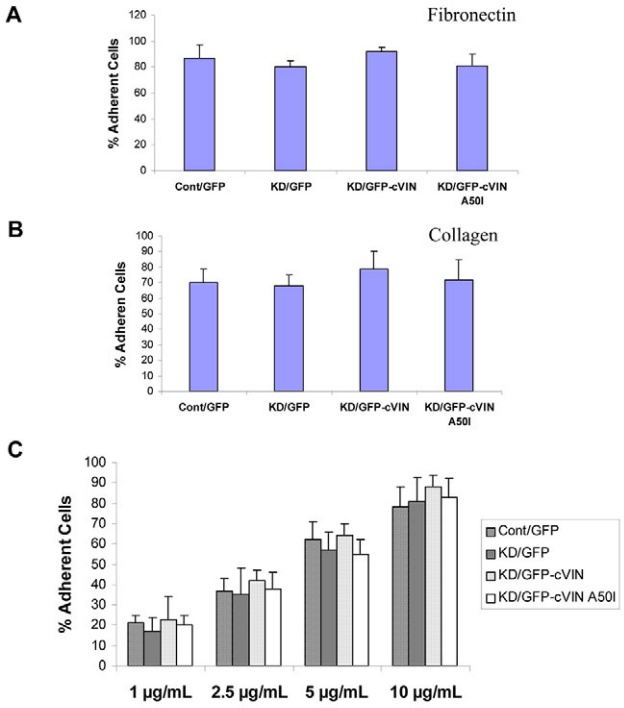

Fig. 3. Phenotypes of vinculin knockdown cells are not due to altered cell-matrix adhesions. Cells were plated on coverslips coated with saturating concentrations of (**A**) fibronectin, (**B**) collagen, or (**C**) sub-saturating concentrations of fibronectin. The coverslips were washed, and the number of adherent cells per field of view (FOV) was counted. Thirty-five FOVs from three independent experiments were quantified and used to calculate the percent of adherent cells. Each bar represents the mean ± s.e.m.

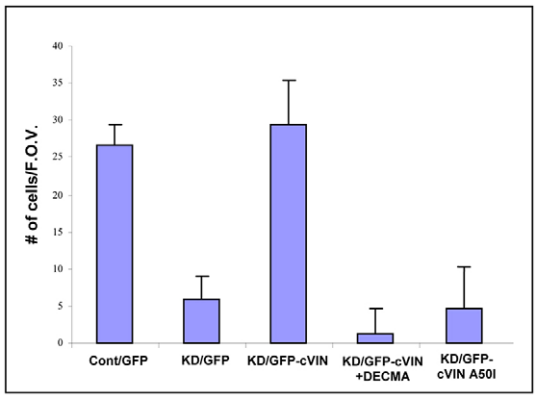

Fig. 4. Adhesion to cadherin extracellular domains is impaired in cells with reduced vinculin levels. For assessing homophilic ligation, dishes were coated with an anti-Fc antibody, washed, coated with human E-cadherin extracellular domains fused to Fc, and blocked with BSA. Cells expressing the indicated constructs were lifted, incubated in the coated dishes, and washed extensively with agitation. Cells were scored as adherent if they were phase gray. The mean number of cells that adhered per field of view ± s.e.m. was calculated by the means of three independent experiments. A sample of the knockdown cells rescued with wild-type vinculin was preincubated with the function-blocking antibody DECMA (+DECMA) prior to plating.

Vinculin depletion reduces E-cadherin levels at the cell surface

The observation that the vinculin knockdown cells did not adhere to or spread well on the cadherin extracellular domains suggested that there was some change in E-cadherin functionality in these cells. We thus used immunofluorescence to examine the localization of E-cadherin in confluent cell monolayers. We found that in the vinculin-depleted cells, the adherens junctions had not formed despite the fact that the cells had been cultured at confluence for several days; the E-cadherin staining pattern was punctate and serrated, and the cytoplasmic levels of E-cadherin were increased (Fig. 5A). The control cells, by contrast, exhibited the characteristic distribution of E-cadherin normally seen in epithelial cells (Fig. 5A). The expression of cVIN rescued the changes in E-cadherin localization and cell morphology, suggesting that these effects are specific to vinculin depletion. In further support of a disruption in cell-cell junctions after vinculin depletion, aberrant localization of β-catenin (Fig. 5B) and actin were also observed (supplementary material Fig. S6).

The immunofluorescence images suggest that E-cadherin is lost from the cell surface in the vinculin knockdown cells. To test this directly, we examined the surface levels of E-cadherin by labeling the cell surface molecules with biotin and examining the amount of labeled E-cadherin in the control and knockdown cells. The vinculin knockdown cells had decreased levels of surface E-cadherin, as compared to control cells and to vinculin knockdown cells rescued with wild-type cVIN (Fig. 6). Under these conditions, the total levels of E-cadherin in various cell types were constant (Fig. 6). These findings demonstrate that vinculin is required for the cell-surface expression of E-cadherin.

The interaction between vinculin and α-catenin is not required for organization of the AJs

To begin to address the mechanism by which vinculin regulates cell-surface expression of E-cadherin, we studied the effects of a mutant version of vinculin (cVIN A50I, in which alanine 50 is substituted by isoleucine) that is unable to bind to some head ligands such as talin (Bakolitsa et al., 2004; Cohen et al., 2006). Like the wild-type vinculin (cVIN), this mutant version of vinculin was insensitive to the shRNAs targeting endogenous vinculin (Fig. 6) when expressed in the vinculin knockdown cells (KD/GFP-cVIN A50I). However, cVIN A50I did not rescue either the morphological changes induced by inhibiting vinculin expression or the loss of cell-surface E-cadherin (Figs 1, 4-6). In some instances (Fig. 6), cVIN A50I was unable to rescue the defects to knockdown levels, suggesting that it might have some dominant-negative properties. cVIN A50I also failed to localize to adherens junctions (Fig. 5). The latter observation was unexpected given that this mutant protein readily localizes to cell-matrix adhesions (Humphries et al., 2007) (supplementary material Fig. S5).

This finding indicates that vinculin localization to adherens junctions occurs via a mechanism that differs from that required for its localization to focal adhesions. One possible explanation for the difference is that a specific ligand binds to vinculin through A50 and localizes the protein to cell-cell junctions. Previous studies suggest that this ligand is α-catenin (Sheikh et al., 2006; Watabe-Uchida et al., 1998), which is present in adherens junctions but not in focal adhesions. Numerous studies support the idea that vinculin binds α-catenin (Bakolitsa et al., 2004; Hazan et al., 1997; Imamura et al., 1999; Subauste et al., 2005; Watabe-Uchida et al., 1998; Weiss et al., 1998; Yamada et al., 2005). Moreover, structural studies with

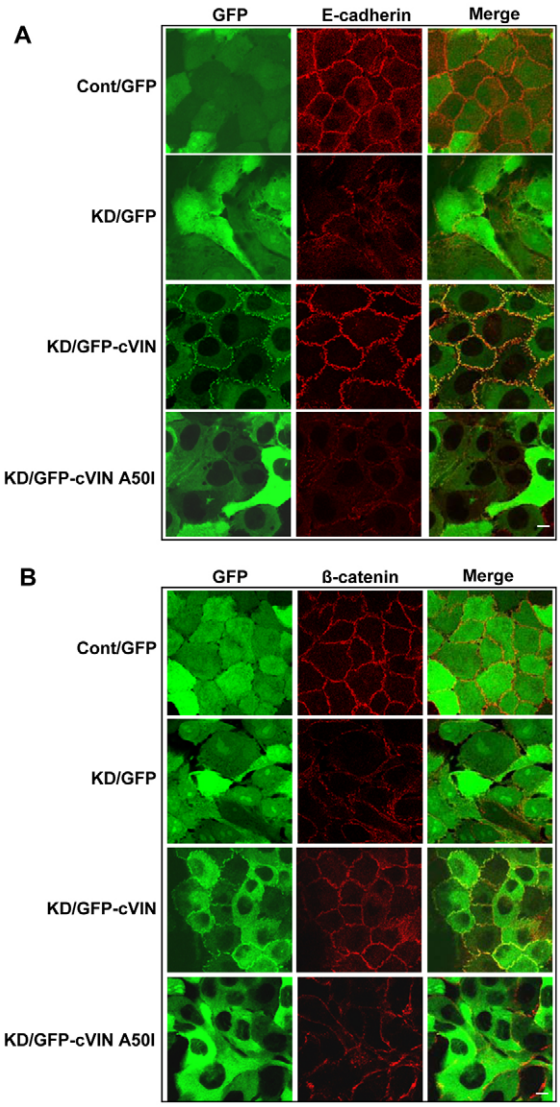

Fig. 5. E-cadherin localization to adherens junctions is altered in cells with low levels of vinculin. MCF10a cells stably expressing the indicated constructs (green) were analyzed by immunofluorescence, following staining with antibodies against (**A**) E-cadherin (red) or (**B**) β-catenin (red). Representative images are shown. Scale bar: 10 µm.

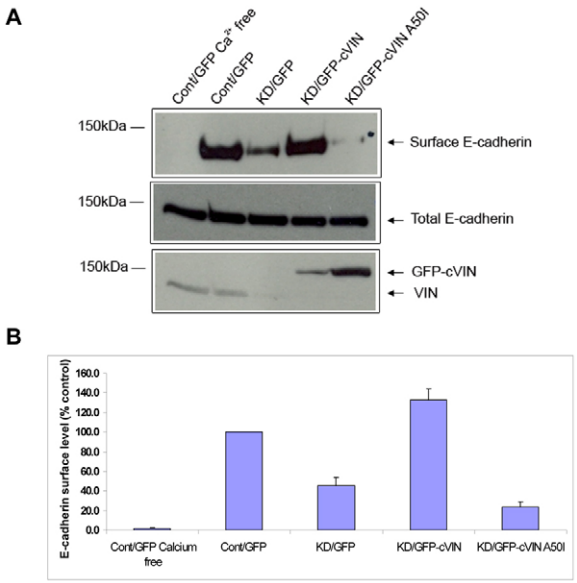

Fig. 6. Vinculin regulates surface expression of E-cadherin. (**A**) Surface E-cadherins were biotinylated. After the reaction was quenched, cells were lysed and the biotinylated proteins were recovered with streptavidin beads. Surface E-cadherin or whole-cell lysates were analyzed by SDS-PAGE and immunoblotted with E-cadherin antibody. In the control experiment (Cont/GFP Ca^{2+} free), cells were first incubated with EGTA to disassemble adherens junctions. (**B**) The amount of E-cadherin on the cell surface was quantified using densitometry. The mean level of E-cadherin on the cell surface in the control cells was set to 100%. Data presented are the mean ± s.e.m. from three independent experiments.

peptides derived from α-catenin indicate that α-catenin could bind to the same groove in the vinculin D1 domain (amino acids 1-258) to which both IpaA and talin bind (Izard et al., 2004). However, when we tested binding of the purified forms of α-catenin and vinculin in vitro or the ability of purified vinculin to pull down α-catenin from cell lysates, we consistently found that α-catenin still binds to cVin A50I, albeit to a lesser extent (Fig. 7A,B and supplementary material Fig. S7). A similar result was observed when we examined the binding of these two proteins in cell lysates (Fig. 7C). The observation that cVIN A50I fails to rescue the vinculin knockdown phenotypes but maintains some ability to bind to α-catenin suggests that only a low level of α-catenin binding is required for the effect of vinculin on junctions, or that another protein is important.

β-catenin binding is required for vinculin effects on E-cadherin

Like α-catenin, β-catenin has been identified as a ligand of the vinculin head domain, and it is highly enriched in adherens junctions (Hazan et al., 1997) (reviewed by Wheelock and Johnson, 2003a; Wheelock and Johnson, 2003b). We thus investigated whether cVIN A50I could block β-catenin binding to vinculin. We failed to observe co-immunoprecipitation of β-catenin and cVIN A50I (Fig. 7D) under conditions in which wild-type cVIN readily bound β-catenin. These findings identify β-catenin as a strong candidate for the ligand that interacts with vinculin to promote the recruitment and/or retention of E-cadherin to sites of cell-cell adhesion. At present, no other vinculin ligands are known to both be present specifically at the adherens junctions in MCF10a cells and to interact with vinculin in an A50-dependent manner.

These observations suggested that an interaction between β-catenin and vinculin is crucial for E-cadherin cell-surface expression. To explore the role of this interaction between β-catenin and vinculin, we considered generating a mutant form of β-catenin that could not bind to vinculin. This would allow us to examine the phenotype of this β-catenin when expressed in cells lacking β-catenin. We mapped the vinculin-binding site on β-catenin using a series of β-catenin fragments expressed as GST fusion proteins (Fig. 8A). β-catenin is comprised of a central armadillo repeat and flexible N- and C-termini. Previous studies suggested that α-catenin and vinculin compete for binding to β-catenin, indicating that the β-catenin N-terminus would be important for interaction with vinculin (Hazan et al., 1997). Using our β-catenin–GST fusions, we found

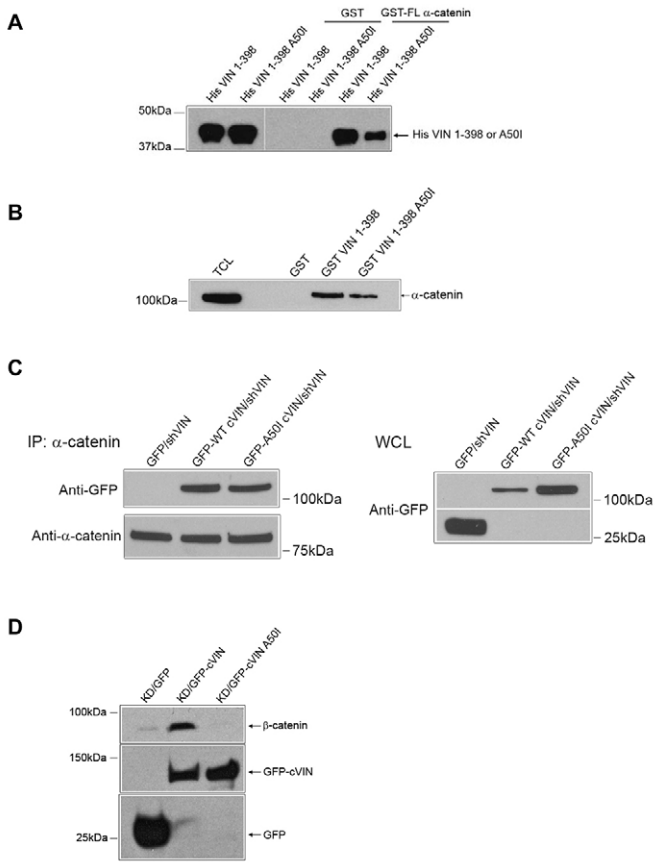

Fig. 7. Substitution of A50I blocks β-catenin binding to vinculin, but not α-catenin. (**A**) In vitro binding analysis of α-catenin interaction with wild-type vinculin (His VIN 1-398) or mutant vinculin (His VIN 1-398 A50I) head sequence encompassing amino acids 1-398. Purified His-VIN or His-VIN A50I were incubated with purified GST or GST-tagged full-length α-catenin at room temperature for 30 minutes, and then recovered using glutathione beads. The beads were washed, after which the bound peptides were separated by SDS-PAGE and immunoblotted with His antibodies. Purified wild-type and mutant peptides were included to indicate the positions of the purified proteins. All of the samples were prepared and analyzed in the same experiment. The white line indicates where the western blot was cut to remove some irrelevant lanes. (**B**) Pull-down analysis of α-catenin interaction with wild-type vinculin (GST VIN 1-398) or mutant vinculin (GST VIN 1-398 A50I) head sequence. Purified GST-VIN or GST-VIN A50I attached to the glutathione beads were incubated with MDCK cell lysates. The beads were then washed, and subjected to western blotting analysis with an antibody against α-catenin. Total cell lysate (TCL) was also included. (**C**) Co-immunoprecipitation of α-catenin with GFP-cVIN or GFP-cVIN A50I. MCF10a cells expressing the indicated construct were lysed, α-catenin was immunoprecipitated, and the immunoprecipitates were recovered using protein A Sepharose. The bound proteins were fractionated by SDS-PAGE and immunoblotted with an antibody against GFP. The blot was stripped and re-probed for α-catenin. The expression levels of GFP-cVIN or GFP-cVIN A50I in the whole cell lysate (WCL) were also shown. (**D**) Co-immunoprecipitation of GFP-cVIN or GFP-cVIN A50I with β-catenin. MCF10a cells expressing the indicated construct were lysed and immunoprecipitated with a GFP antibody. The proteins were then recovered using protein G Sepharose. The beads were washed and fractionated by SDS-PAGE, and immunoblotted with an antibody against β-catenin. The blot was stripped and re-probed for GFP.

that the vinculin-binding site resides in the N-terminal 23 amino acids of β-catenin. This region of β-catenin has been predicted to contain one α-helix (data not shown). Alignment of other vinculin binding sites in talin, IpaA and α-actinin revealed that all these proteins share a similar amphipathic α-helix and several conserved hydrophobic residues (Bois et al., 2005; Izard et al., 2004; Izard et al., 2006). The α-helix of β-catenin that binds to vinculin also has this amphipathic pattern, although the hydrophobic residues are less conserved. Mutation of methionine 8, one of the hydrophobic residues in the α-helix, to proline blocked vinculin binding; this was the case for both the N-terminal fragment and full-length β-catenin (Fig. 8B,C). Pull-down assays using purified full-length wild-type or mutant β-catenin revealed that M8P β-catenin (in which methionine 8 is substituted by proline) specifically blocks vinculin binding while leaving α-catenin binding intact (Fig. 8C). Also, we were able to confirm that the M8P mutant was phosphorylated like the wild-type molecule (supplementary material Fig. S8). The α-catenin binding site (as well as several β-catenin key phosphorylation sites) is known to reside in the N-terminus of β-catenin, which suggests that the M8P amino acid substitution does not affect β-catenin protein folding and function.

We then characterized the M8P mutant by silencing endogenous β-catenin in MCF10a cells and re-expressing wild-type or M8P mutant forms of GFP-tagged mouse β-catenin (Fig. 9A) (Cho et al., 2006; Verma et al., 2003). We first tested whether substitution of M8P disrupted β-catenin association with the vinculin or E-cadherin. As expected, the M8P mutant, but not the wild type β-catenin, prevented vinculin association with E-cadherin (Fig. 9B) but had no effect on β-catenin binding to E-cadherin (Fig. 9C).

We next examined E-cadherin localization in these cells using immunofluorescence. The β-catenin knockdown cells (βKD/GFP) had disrupted adherens junctions with serrated E-cadherin staining, and mutant β-catenin (βKD/GFP-mβcat M8P) failed to rescue this phenotype like the wild-type molecule (βKD/GFP-mβcat) (Fig. 9D). Also, we observed more cytoplasmic staining with the M8P mutant in the β-catenin knockdown cells. However, when M8P localization was examined in cells expressing wild-type levels of β-catenin, both the wild-type and mutant GFP–β-catenins localized to adherens junctions to similar extents (supplementary material Fig. S9). Similar to the vinculin knockdown or rescue cells, we did not observe any change of total E-cadherin level in the β-catenin knockdown or wild-type, or mutant β-catenin rescued cells (Fig. 9E and data not shown). Finally, to test our hypothesis that β-catenin binds vinculin in order to stabilize E-cadherin at sites of cell-cell adhesion, we analyzed E-cadherin surface expression in the newly generated cell lines. Indeed, β-catenin knockdown cells and their β-catenin M8P-expressing counterparts had the same phenotype as the vinculin knockdown cells (decreased surface E-cadherin expression), and this defect was rescued by the expression of wild-type β-catenin (Fig. 9E,F). Taken together, these biochemical and cellular data lead to a new insight on vinculin function at adherens junctions, namely that vinculin regulates surface E-cadherin expression through its interaction with β-catenin.

Discussion

Scores of studies have demonstrated vinculin localization to adherens junctions and support the idea that it is important for cell-cell junctions. Nonetheless, a function for vinculin at this site has remained elusive. We initially attempted to study vinculin function in adherens junction using an overexpressed GFP-tagged vinculin. This approach failed to produce any insight because GFP-vinculin does not readily integrate into mature adhesions in cells with endogenous levels of vinculin. Instead, we turned to a knockdown add-back approach that has been successfully employed by other

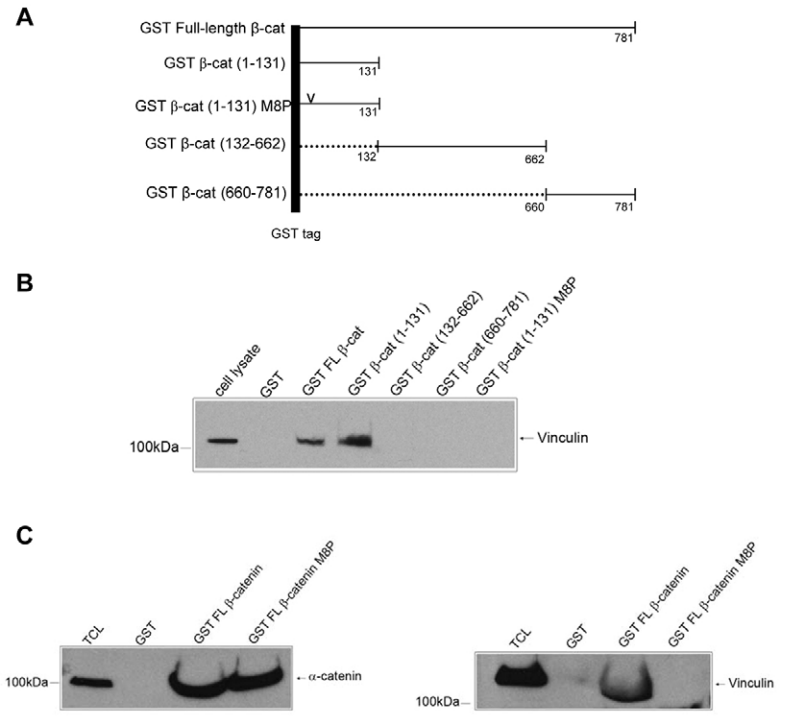

Fig. 8. Substitution of M8P in β-catenin blocks vinculin binding. (**A**) Schematic of β-catenin truncations and the M8P mutation (v). (**B**) Pull-down analysis to map vinculin binding site on β-catenin. Purified GST protein or GST-tagged β-catenin (β-cat) fragments attached to the glutathione beads were incubated with MDCK cell lysates. The beads were washed and fractionated by SDS-PAGE and immunoblotted with vinculin. (**C**) Pull down analysis of α-catenin or vinculin interaction with wild-type β-catenin (GST FL β-catenin) or mutant β-catenin (GST FL β-catenin M8P). Purified GST FL β-catenin or GST FL β-catenin M8P attached to the glutathione beads were incubated with MDCK cell lysates. The beads were then washed and fractionated by SDS-PAGE, and immunoblotted with an antibody against α-catenin or vinculin. Total cell lysate (TCL) was also included.

laboratories. The vinculin knockdown cells we generated are characterized by altered cell-cell adhesions (Figs 4-6), despite adhering normally to the extracellular matrix (Figs 2, 3). The morphological changes we observed are a loss of the honeycomb shape (Fig. 1B) – alterations that are reminiscent of those found in transformed cells (Kawahara et al., 1999; Lifschitz-Mercer et al., 1997; Meyer and Brinck, 1997; Sadano et al., 1992; Somiari et al., 2003) – and they result from a reduction in cell-surface E-cadherin expression and a consequent loss of cell-cell adhesion (Figs 4-6). We have investigated the mechanism responsible for the effects of vinculin loss and have found that vinculin must be able to associate with β-catenin physically in order to regulate surface cadherin levels. Thus, vinculin regulates cell-surface E-cadherin expression by binding to β-catenin.

How does vinculin regulate E-cadherin levels at the cell surface? One possibility is that the vinculin acts much like p120 catenin, which reduces E-cadherin surface levels by targeting it for degradation. This mechanism is not plausible given that the total levels of E-cadherin are unaffected by silencing of vinculin. An alternative possibility is that the vinculin–β-catenin interaction is required for transport of E-cadherin to the cell surface. This idea seems highly unlikely given that the pool of vinculin that is active in a cell is predominantly localized to the plasma membrane (Chen et al., 2005). Our favorite hypothesis is that vinculin acts much as it does to promote cell-matrix adhesions, where it increases the stability of focal adhesions (Coll et al., 1995; Saunders et al., 2006; Xu et al., 1998a) by controlling the lifetime of vinculin-talin complexes (Humphries et al., 2007). We found that in cell-cell junctions vinculin regulates cell-surface expression of E-cadherin by binding β-catenin (Fig. 9). Thus, vinculin could regulate the lifetime of protein complexes at the cadherin cytoplasmic tail in much the same manner as it regulates integrin supramolecular protein complexes in focal adhesions (Saunders et al., 2006; Humphries et al., 2007). In support of this idea, there are some similarities between losses of vinculin in the two sites. For example, in both contexts, vinculin depletion is accompanied by dramatic reduction in cell adhesion. This decrease manifests itself in the form of fewer and smaller adhesions in cell-matrix adhesions (Saunders et al., 2006; Humphries et al., 2007) and a global disruption of cell-cell adhesions (Figs 4, 5). It is not known whether integrin levels are altered in fibroblasts lacking vinculin, but this investigation might be warranted in the light of the findings presented here.

Historically, α-catenin was thought to recruit vinculin to cell-cell junctions because vinculin was lost from adherens junctions in cancer cells or in hearts lacking α-catenin (Sheikh et al., 2006; Watabe-Uchida et al., 1998). However, in other cancer cell lines lacking α-catenin, vinculin could be co-immunopreciptitated with β-catenin–E-cadherin complexes (Hazan et al., 1997). Our experiments indicate a requirement of β-catenin for localization of vinculin to cell-cell junctions. This idea is supported by two observations. The first is that a mutant version of vinculin that retains its ability to bind α-catenin, but not β-catenin, was impaired in junctional localization (Figs 5, 7). Second, shRNA-mediated inhibition of β-catenin expression resulted in a phenotype that was reminiscent of those obtained in the vinculin knockdown cells and, importantly, this phenotype could not be rescued by a mutant version of β-catenin that cannot associate with vinculin (Fig. 9). One possible explanation for these differences is that, in some contexts, α-catenin manifested itself as important for vinculin due to its effects on β-catenin. This notion is supported by the observation that the form of β-catenin that binds preferentially to cadherin also binds α-catenin, and that pre-association of recombinant α-catenin with β-catenin leads to enhanced binding of β-catenin to cadherin (Castano et al., 2002). In our cell lines, α-catenin expression is not disturbed (data not shown), and our mutant version of β-catenin that does not bind vinculin retains its ability to associate with α-catenin to wild-type levels (Fig. 8D). These observations indicate that if α-catenin is required, it is secondary to β-catenin or is part of a molecular apparatus (including β-catenin) that is important for vinculin localization.

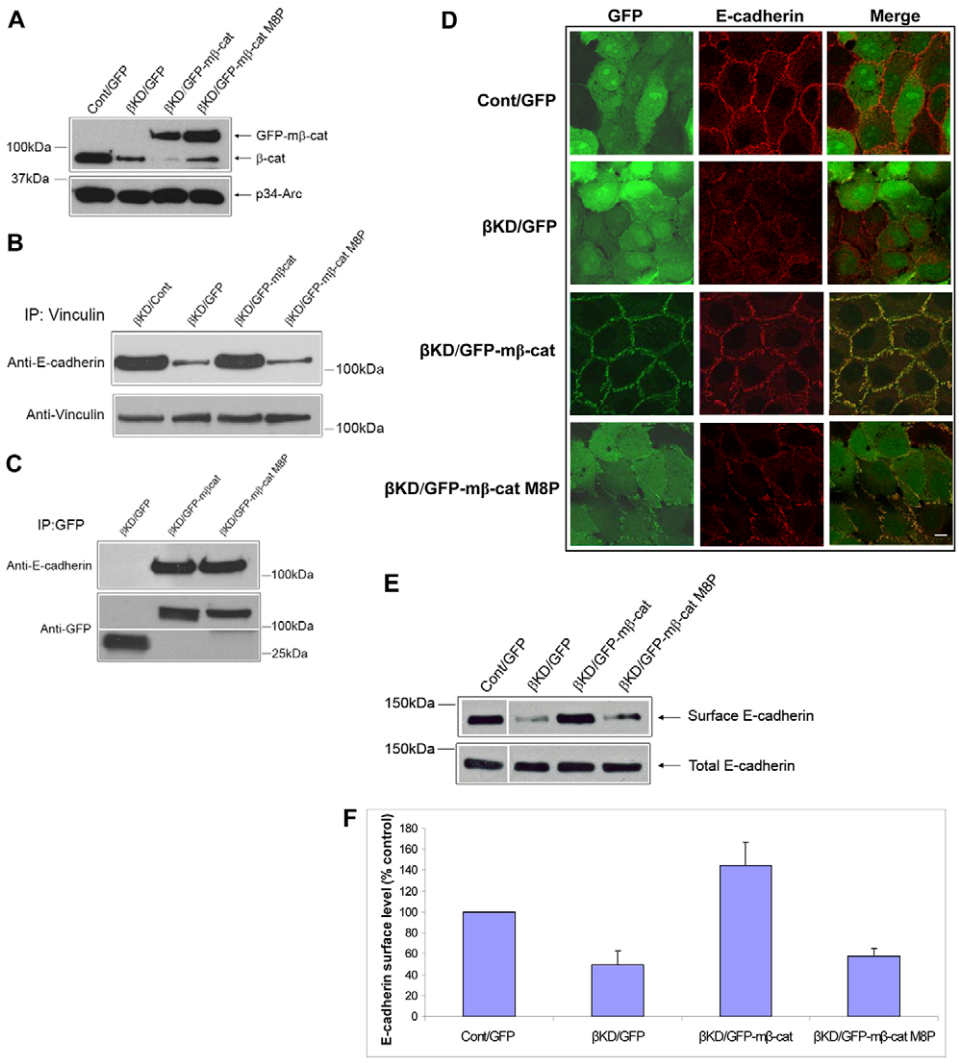

Fig. 9. Vinculin binding to β-catenin is required for cell surface E-cadherin expression. (**A**) Representative blots of MCF10a cells stably expressing the indicated constructs. Lysates were harvested from cell lines, and western blot analysis was performed using antibodies against vinculin (VIN) or the p34-Arc subunit of the Arp2/3 complex as a loading control (βKD, β-catenin knockdown; mβ-cat, mouse β-catenin). (**B**) Co-immunoprecipitation of vinculin with E-cadherin. MCF10a cells expressing the indicated construct were lysed and immunoprecipitated with a vinculin antibody. The proteins were then recovered using protein G Sepharose. The beads were washed and fractionated by SDS-PAGE, and immunoblotted with an antibody against E-cadherin. The blot was stripped and re-probed for vinculin. (**C**) Co-immunoprecipitation of GFP-mβ-catenin or GFP-mβ-catenin M8P with E-cadherin. MCF10a cells expressing the indicated construct were lysed and immunoprecipitated with a GFP antibody. The proteins were then recovered using protein G Sepharose. The beads were washed and fractionated by SDS-PAGE, and immunoblotted with an antibody against E-cadherin. The blot was stripped and re-probed for GFP. (**D**) MCF10a cells stably expressing the indicated GFP-proteins (green) were analyzed by carrying out immunofluorescence analysis with antibodies against E-cadherin (red). Representative images are shown. Scale bar: 10 μm. (**E**) The presence of E-cadherin at the surface in indicated cell lines was identified by surface biotinylation as described in Fig. 6. All of the samples were prepared and analyzed in the same experiment; the white line indicates where the western blot was cut to remove some irrelevant lanes. (**F**) Quantification of E-cadherin levels at the surface by comparison to the control cells. Data were obtained at described in Fig. 6 and are representative of three independent experiments.

More recent work has implicated myosin VI in vinculin recruitment to cell-cell junctions. Specifically, myosin VI was found to be necessary for incorporation of vinculin into stable cadherin-containing adhesions (Maddugoda et al., 2007). In this work, it was noted that the arrival of vinculin at cell-cell adhesions preceded the time at which myosin VI was detected at these sites (Maddugoda et al., 2007). This observation, combined with our finding that vinculin recruitment requires β-catenin, suggests the intriguing possibility that the initial recruitment of vinculin to cell-cell adhesions is mediated by β-catenin, and that myosin VI is dominant at a later stage.

We have discovered that vinculin stabilizes E-cadherin on the cell surface by virtue of its ability to bind β-catenin. This important stabilizing function requires vinculin to bind the β-catenin N-terminus because mutant versions of β-catenin lacking the N-terminal or harboring a M8P substitution are unable to bind vinculin and, in the latter case, are unable to rescue cell-surface expression of E-cadherin defects. This domain has been implicated in regulating β-catenin at adherens junctions. It binds a number of proteins that regulate the transition of cancer cells from an epithelial to a more mesenchymal phenotype (Lal et al., 2008; Stemmer et al., 2008). The β-catenin N-terminus also contains a number of phosphorylation

sites that dictate how rapidly β-catenin is degraded (Daugherty and Gottardi, 2007). Finally, there is some evidence that this region regulates the affinity of β-catenin for E-cadherin, α-catenin and other binding partners involved in cell adhesion (Castano et al., 2002; Piedra et al., 2001; Pokutta and Weis, 2000). For example, the use of N-terminal deletion mutants lacking amino acid residues 1-119 has identified this region in regulating the affinity of β-catenin for its various ligands (Castano et al., 2002). However, another study did not support a role for the N-terminus in the affinity of β-catenin for E-cadherin (Choi et al., 2006). Neither study employed vinculin or a combination of vinculin and another binding partner, so we do not yet know if an interaction with vinculin can change the affinity of β-catenin for E-cadherin. Our observation that the M8P version of β-catenin co-precipitates with E-cadherin to wild-type levels is consistent with the idea that vinculin is not required for this interaction. However, we cannot rule out the possibility that the assay employed in our studies is not sensitive enough to detect small affinity changes in the tight interaction between E-cadherin and β-catenin (pmol to nmol affinity) (Choi et al., 2006). If vinculin does not regulate the association of β-catenin with E-cadherin as our data suggests, then we would predict that it might serve to stabilize this complex at the plasma membrane.

Another interesting finding that emerged from the studies examining vinculin function in adherens junctions is that there are some striking differences from those in focal adhesions. Although vinculin localization to focal adhesions is not fully understood, it is clear that vinculin alanine 50 is not required (Humphries et al., 2007). By contrast, in the case of adherens junctions, the cVin A50I mutant is unable to localize correctly, underscoring the importance of this residue (Fig. 4). Moreover, β-catenin, a protein that is not present in focal adhesions, is required for vinculin recruitment to the cadherin adhesion complex. Less is known with respect to how vinculin is activated each site. Talin is known to activate vinculin in focal adhesions, but it is not present in adherens junctions. Hence it seems likely that one of previously identified vinculin ligands (β-catenin, α-catenin and/or myosin VI) provides this important function. More work is needed for a complete understanding of how vinculin is directed to and activated in one adhesion site versus the next.

In summary, we show that cell-surface expression of E-cadherin is regulated by vinculin binding to β-catenin. This observation suggests that cadherin adhesiveness is modulated, in part, by signaling events that dynamically influence vinculin binding to β-catenin. There is a well-established link between the loss of vinculin from adhesion sites and advanced histologic grade and poor survival rates in patients suffering from cancers that are epithelial in origin (Glukhova et al., 1995; Kuroda et al., 2000; Kuroda et al., 2001; Lifschitz-Mercer et al., 1997; Raz et al., 1986; Wiebe et al., 2000). The findings presented herein indicate that the poor outcomes faced by these individuals might be in part due to a loss in their ability to regulate the tumor-suppressive effect of E-cadherin.

Materials and Methods

Constructs

pSUPER-shVIN, pSUPER-shβcat or pSUPER-scramble were constructed by subcloning custom oligos designed to hybridize to human vinculin, human β-catenin or scramble of the vinculin-targeting sequence into the retroviral vector, pSUPER-RETRO-PURO (Oligoengine). pLEGFP-WT vinculin was generated by amplifying the full-length chick vinculin sequence, ligating it into pENTR-DTOPO (Invitrogen) and then cloning it into a pLEGFP DEST vector using the Gateway recombinational cloning system (Invitrogen). The pLEGFP DEST vector was derived from the pLEGFP-C1 vector (Clontech), which is Gateway compatible, by digesting with *Hin*dIII and *Bam*HI, eliminating the overhanging sequence, and ligating the resulting DNA into Reading Frame Cassette A according to the manufacturer's protocol (Invitrogen). pLEGFP-WT β-catenin was generated by cutting pGEX-KG-WT mβ-catenin (a generous gift of Jim Lin, University of Iowa, Iowa City, IA) (Choi et al., 2007) with *Bam*HI and *Sal*I, and ligating it into pLEGFP-C1 vector cut with the same enzymes. pLEGFP-vinculin A50I or pLEGFP-β-catenin M8P was prepared using site-specific mutagenesis to introduce the appropriate single amino-acid substitution into pLEGFP-WT vinculin or pLEGFP-WT β-catenin. pGEX4T1-FL α-catenin is a full-length human α-catenin cDNA fused in-frame with GST, and was a generous gift from David Rimm (Yale University, New Haven, CT). pET28a-vinculin 1-398, pGEX4T1-vinculin 1-398 (a generous gift of David Critchley, University of Leicester, Leicester, UK) or pGEX4T1-β-catenin truncations (Fig. 8) were constructed by PCR amplification of corresponding residues of chick vinculin or mouse β-catenin and subcloning these into pET28a (Novagen) or pGEX4T1 (GE-Healthcare). pET28a-vinculin 1-398 A50I, pGEX4T1-vinculin 1-398 A50I, and pGEX4T1-β-catenin (1-131) M8P were prepared by using site-specific mutagenesis to introduce a mutation resulting in the appropriate single amino-acid substitution into pET28a-vinculin 1-398, pGEX4T1-vinculin 1-398 and pGEX4T1-β-catenin (1-131).

Cell lines

MCF10a human breast epithelial cells (ATCC) were maintained in DMEM/F12 (1:1) medium supplemented with 5% horse serum, 1% penicillin-streptomycin, 20 ng/ml epidermal growth factor, 0.5 mg/ml hydrocortisone, 100 ng/ml cholera toxin and 10 μg/ml insulin. 293GPG cells were maintained in DMEM medium supplemented with 10% heat-inactivated FBS, 1% penicillin-streptomycin, 2 mM L-glutamine, 1 μg/ml tetracycline, 2 μg/ml puromycin, 0.3 mg/ml G418 and 20 mM HEPES. During retrovirus production, 293GPG cells were maintained in virus-producing medium (DMEM medium supplemented with 10% heat-inactivated FBS, 1% penicillin-streptomycin, 2 mM L-glutamine and 20 mM HEPES). Caco-2 cells (ATCC) were maintained in Eagle's minimum essential medium supplemented with 20% FBS and 1% penicillin-streptomycin.

Packaging of retroviral constructs and infection of MCF10a

293GPG cells were transfected with pLEGFP-C1 vector, pLEGFP-WT vinculin, pLEGFP-vinculin A50I, pLEGFP-WT β-catenin, pLEGFP-β-catenin M8P, pSUPER-RETRO or pSUPER-shVIN using Lipofectamine reagent (Invitrogen) as previously described (Ory et al., 1996; DeMali et al., 1999). MCF10a cells stably expressing GFP, GFP-tagged vinculin, or GFP-tagged β-catenin were selected in 0.5 mg/ml G418 and were infected a second time with retrovirus containing the empty vector (pSUPER-RETRO), scramble sequence (pSUPER-scramble), pSUPER-shVIN or pSUPER-shβcat. Doubly infected MCF10a cells were selected in 0.5 mg/ml G418 and 2 μg/ml puromycin. Caco-2 cells stably expressing pSUPER-RETRO or pSUPER-shVIN were selected in 2.5 μg/ml puromycin.

Immunoprecipitation and western blotting

Cells were washed twice in HEPES buffered saline extraction buffer (20 mM HEPES, pH 7.4, 150 mM NaCl), and lysed in ice-cold buffer [1% Triton X-100, 10 mM Tris-HCl, pH 7.4, 5 mM EDTA, 50 mM NaCl, 50 mM NaF, 0.1% BSA, 20 μg/ml aprotinin, 2 mM Na_3VO_4 and 1 mM phenylmethylsulfonyl fluoride (PMSF)] or GFP immunoprecipitation buffer (50 mM Tris-HCl, pH 7.6, 150 mM NaCl, 1% NP-40, 0.5% deoxycholate, 20 μg/ml aprotinin, 2 mM Na_3VO_4 and 1 mM PMSF). GFP was immunoprecipitated with a monoclonal GFP antibody (Roche), vinculin was immunoprecipitated with a monoclonal vinculin antibody (hVIN-1, Sigma) and α-catenin was immunoprecipitated with a rabbit polyclonal antibody raised against human/mouse α-catenin amino acids 890-901 (Sigma). Immunoprecipitates were washed four times in GFP-immunoprecipitation buffer, fractionated by SDS-PAGE, transferred to PVDF and subjected to western blot analysis. For the analysis of vinculin levels in the different shRNA knockdown cells, lysate aliquots with equal amounts of total protein (as measured using the Pierce Coomassie protein assay reagent) were separated on an SDS-PAGE gel. Western blotting was then performed with the appropriate antibody: vinculin was blotted using a rabbit antibody raised against purified chick gizzard vinculin (DeMali et al., 2002). The p34-Arc subunit of the Arp2/3 complex was blotted using a rabbit polyclonal antibody raised against a peptide that encompassed amino acids 179-204 of p34-Arc (DeMali et al., 2002). α-catenin was blotted with a rabbit polyclonal antibody raised against human/mouse α-catenin amino acids 890-901 (Sigma); β-catenin was blotted with a rabbit polyclonal antibody raised against human/mouse β-catenin amino acids 768-781 (Sigma). E-cadherin was blotted with an HECD-1 mouse monoclonal antibody (Calbiochem). GFP was blotted with a mouse monoclonal antibody (Roche). Actin was blotted with a mouse monoclonal antibody (clone C4, MP Biomedicals). The blots were developed using ECL western blot detection reagents (Pierce), and the signal was detected on X-ray film (Kodak).

Immunofluorescence

Cells were fixed in 3.7% formaldehyde in phosphate buffered saline (PBS), permeabilized in 0.5% Triton X-100 in universal buffer (UB; 150 mM NaCl, 50 mM Tris pH 7.6, 0.01% NaN_3) for 3 minutes, and washed in UB. Cells were blocked with 1% BSA in UB for E-cadherin and β-catenin staining or with 10% BSA in UB for vinculin and paxillin staining for 30 minutes at 37°C, incubated with a primary antibody for 45 minutes at 37°C, washed, and incubated with secondary antibody

for 45 minutes at 37°C. E-cadherin was visualized by staining with HECD-1 (Calbiochem) at a 1:1000 dilution, followed by Texas-red-conjugated goat anti-mouse IgG (H+L) (Jackson ImmunoResearch Laboratories) at a 1:500 dilution. Vinculin was visualized using FITC-conjugated hVIN-1 (Sigma) at 1:50, or hVIN-1 (Sigma) at a 1:200 dilution, followed by Texas-red-conjugated donkey anti-mouse IgG (H+L) (Jackson ImmunoResearch Laboratories) at a 1:200 dilution. β-catenin was visualized using the rabbit polyclonal antibody (Sigma) at 1:300 dilution. Actin was visualized using Texas-red-conjugated phalloidin (Invitrogen) at a 1:750 dilution. Paxillin was visualized using TRITC-conjugated mouse antibody (BD Transduction Laboratories). Fluorescence images were captured at room temperature with a confocal microscope (model LSM 510; Carl Zeiss MicroImaging). We used a 63× oil objective (Carl Zeiss MicroImaging) with an NA of 1.4. Images were obtained using the LSM Image Browser (Carl Zeiss MicroImaging). Phase images were captured at room temperature with an Axiovert 200M inverted microscope (Carl Zeiss MicroImaging), equipped with an ORCA-ERA 1394 HD camera (Hamamatsu Corporation). A 10× EC Plan Neofluor objective (Carl Zeiss MicroImaging) with an NA of 0.55 was employed for these studies. Images were acquired using Axiovision 4.7 software (Carl Zeiss MicroImaging). The intensity of vinculin, β-catenin and paxillin fluorescence at cell-cell contacts was measured as described (Maddugoda et al., 2007). Briefly, ImageJ was used to quantify the mean pixel intensity of vinculin, β-catenin or paxillin staining at junctions. Background was subtracted using a region with identical area for each contact quantified. Fluorescence intensity of vinculin staining was expressed as a ratio of the β-catenin or paxillin fluorescence intensity. The fluorescence intensity of β-catenin or paxillin was not significantly altered between the control and knockdown cells. Experiments were performed three times with 30 contacts analyzed per experiment. Data shown are representative of three independent experiments.

Transmission electron microscopy

Confluent cells growing on 0.4 μm Transwell filters were fixed in 2.5% gluteraldehyde in 0.1 M cacodylate buffer. After rinses in 0.1 M cacodylate buffers, cells were processed for transmission electron microscopy by using routine procedures. Ultrathin sections were prepared and imaged in a JEOL JEM-1230 transmission electron microscope equipped with a Gatan Ultrascan 2k × 2k CCD camera.

Determination of growth rates

To measure the doubling time of each cell line, 2.5×10^4 cells were seeded into a 35-mm dish. For 9 consecutive days, one well of cells was trypsinized and counted every day. The cell doubling time was determined by plotting the number of cells counted against the hours and calculated as the mean of three independent experiments.

Surface biotinylation

Cells were grown to confluence on Transwell filters, washed three times in Ringer's buffer (10 mM HEPES, pH 7.4, 154 mM NaCl, 7.2 mM KCl), and then labeled with 500 μg/mL sulfo-NHS-biotin (Pierce) for 20 minutes at 4°C. The biotinylation reaction was quenched by incubating the cells with five washes of Ringer's buffer containing BSA and NH_4Cl. The cells were lysed in RIPA buffer (50 mM Tris-HCl, pH 7.5, 1% NP-40, 0.25% sodium deoxycholate, 150 mM NaCl, 1 mM EDTA, 20 μg/ml aprotinin, 1 mM PMSF and 2 mM Na_3VO_4) and centrifuged to remove the insoluble fraction. The biotinylated proteins were then recovered using streptavidin agarose. The beads were washed three times with high-stringency buffer (0.1% SDS, 0.5% sodium deoxycholate, 0.5% Triton X-100, 20 mM Tris-HCl, pH 7.5, 120 mM NaCl, 25 mM KCl, 5 mM EDTA and 5 mM EGTA) followed by three washes with low-salt wash buffer (2 mM EDTA, 10 mM Tris-HCl, pH 7.5, 0.5 mM dithiothreitol), fractionated by SDS-PAGE and transferred to PVDF membranes. Total and cell-surface E-cadherin levels were examined by western blotting.

Protein purification

Recombinant GST, GST-FL α-catenin, GST-vinculin 1-398, GST-vinculin 1-398 A50I, GST-FL β-catenin, GST-FL β-catenin M8P, GST-β-catenin truncations, His6-tagged vinculin 1-398, His6-tagged vinculin 1-398 A50I were purified by affinity chromatography. After elution, GST and GST-FL α-catenin were dialyzed against a modified UB buffer containing 10 mM Tris-HCl at pH 7.6 and 100 mM NaCl, whereas His6-tagged vinculin 1-398 and A50I were dialyzed against PBS. Proteins were concentrated using the Amicon Ultra 30,000 MWCO system (Millipore) and stored at 4°C.

in vitro binding assay

Purified GST or GST-FL α-catenin (4.5 μM) was incubated with 1.0 μM His6-vinculin 1-398 or His6-vinculin 1-398 A50I in binding buffer (20 mM Tris-HCl, pH 7.0, 100 mM KCl, 0.2 mM EGTA, 4 mM $MgCl_2$, 0.5 mM dithiothreitol, 20 μg/ml aprotinin and 1 mM PMSF) at room temperature for 30 minutes. The mixture was then incubated with glutathione-Sepharose that had been pre-incubated with 5 μM BSA at 4°C for 30 minutes. The recovered proteins were washed, fractionated by SDS-PAGE and analyzed by western blotting.

Pull-down assays

50 μg of purified GST, GST-vinculin 1-398, GST-vinculin 1-398 A50I, GST-FL β-catenin or GST-β-catenin truncations bound to the glutathione-Sepharose were incubated with MDCK cell lysate at 4°C for 1.5 hours. The recovered proteins were washed, fractionated by SDS-PAGE and analyzed by western blotting.

Adhesion assays

Adhesion to cadherin extracellular domains was tested and quantified as previously described (Noren et al., 2001). Adhesion of cells to fibronectin or collagen was tested and quantified as previously described (DeMali et al., 2002).

We would like to thank David Critchley, David Rimm and Jim Lin for the generous gift of reagents, and Peter Rubenstein for comments on the manuscript. We are especially grateful to Susan Criag for advice, critical comments on the manuscript, and for sharing her initial observation with us that α-catenin binds A50I vinculin. We thank Keith Burridge for allowing the initial phases of this project to be carried out in his laboratory, and Thomas Moninger in the Central Microscopy Facility at the University of Iowa for his help in completing the transmission EM studies.

This work is supported by National Institutes of Health Grant #1K01CA111818 and American Cancer Society Research Scholar Grant #115274 to K.A.D., and American Heart Association Predoctoral Fellowship #0910127G to X.P. Deposited in PMC for release after 12 months.

Supplementary material available online at
http://jcs.biologists.org/cgi/content/full/123/4/567/DC1

References

Bakolitsa, C., Cohen, D. M., Bankston, L. A., Bobkov, A. A., Cadwell, G. W., Jennings, L., Critchley, D. R., Craig, S. W. and Liddington, R. C. (2004). Structural basis for vinculin activation at sites of cell adhesion. *Nature* **430**, 583-586.

Barth, A. I., Nathke, I. S. and Nelson, W. J. (1997). Cadherins, catenins and APC protein: interplay between cytoskeletal complexes and signaling pathways. *Curr. Opin. Cell Biol.* **9**, 683-690.

Bois, P. R., Borgon, R. A., Vonrhein, C. and Izard, T. (2005). Structural dynamics of alpha-actinin-vinculin interactions. *Mol. Cell. Biol.* **25**, 6112-6122.

Bryant, D. M. and Stow, J. L. (2004). The ins and outs of E-cadherin trafficking. *Trends Cell Biol.* **14**, 427-434.

Burridge, K. and Feramisco, J. R. (1980). Microinjection and localization of a 130K protein in living fibroblasts: a relationship to actin and fibronectin. *Cell* **19**, 587-595.

Castano, J., Raurell, I., Piedra, J. A., Miravet, S., Dunach, M. and Garcia de Herreros, A. (2002). Beta-catenin N- and C-terminal tails modulate the coordinated binding of adherens junction proteins to beta-catenin. *J. Biol. Chem.* **277**, 31541-31550.

Chen, H., Cohen, D. M., Choudhury, D. M., Kioka, N. and Craig, S. W. (2005). Spatial distribution and functional significance of activated vinculin in living cells. *J. Cell Biol.* **169**, 459-470.

Chen, H., Choudhury, D. M. and Craig, S. W. (2006). Coincidence of actin filaments and talin is required to activate vinculin. *J. Biol. Chem.* **281**, 40389-40398.

Chen, Y. T., Stewart, D. B. and Nelson, W. J. (1999). Coupling assembly of the E-cadherin/beta-catenin complex to efficient endoplasmic reticulum exit and basal-lateral membrane targeting of E-cadherin in polarized MDCK cells. *J. Cell Biol.* **144**, 687-699.

Cho, H. H., Kim, Y. J., Kim, S. J., Kim, J. H., Bae, Y. C., Ba, B. and Jung, J. S. (2006). Endogenous Wnt signaling promotes proliferation and suppresses osteogenic differentiation in human adipose derived stromal cells. *Tissue Eng.* **12**, 111-121.

Choi, H. J., Huber, A. H. and Weis, W. I. (2006). Thermodynamics of beta-catenin-ligand interactions: the roles of the N- and C-terminal tails in modulating binding affinity. *J. Biol. Chem.* **281**, 1027-1038.

Choi, S., Gustafson-Wagner, E. A., Wang, Q., Harlan, S. M., Sinn, H. W., Lin, J. L. and Lin, J. J. (2007). The intercalated disk protein, mXinalpha, is capable of interacting with beta-catenin and bundling actin filaments [corrected]. *J. Biol. Chem.* **282**, 36024-36036.

Cohen, D. M., Chen, H., Johnson, R. P., Choudhury, B. and Craig, S. W. (2005). Two distinct head-tail interfaces cooperate to suppress activation of vinculin by talin. *J. Biol. Chem.* **280**, 17109-17117.

Cohen, D. M., Kutscher, B., Chen, H., Murphy, D. B. and Craig, S. W. (2006). A conformational switch in vinculin drives formation and dynamics of a talin-vinculin complex at focal adhesions. *J. Biol. Chem.* **281**, 16006-16015.

Coll, J. L., Ben-Ze'ev, A., Ezzell, R. M., Rodriguez Fernandez, J. L., Baribault, H., Oshima, R. G. and Adamson, E. D. (1995). Targeted disruption of vinculin genes in F9 and embryonic stem cells changes cell morphology, adhesion, and locomotion. *Proc. Natl. Acad. Sci. USA* **92**, 9161-9165.

Daugherty, R. L. and Gottardi, C. J. (2007). Phospho-regulation of beta-catenin adhesion and signaling functions. *Physiology (Bethesda)* **22**, 303-309.

Davis, M. A., Ireton, R. C. and Reynolds, A. B. (2003). A core function for p120-catenin in cadherin turnover. *J. Cell Biol.* **163**, 525-534.

DeMali, K. A., Balciunaite, E. and Kazlauskas, A. (1999). Integrins enhance platelet-derived growth factor (PDGF)-dependent responses by altering the signal relay enzymes that are recruited to the PDGF beta receptor. *J. Biol. Chem.* **274**, 19551-19558.

DeMali, K. A., Barlow, C. A. and Burridge, K. (2002). Recruitment of the Arp2/3 complex to vinculin: coupling membrane protrusion to matrix adhesion. *J. Cell Biol.* **159**, 881-891.

Geiger, B. (1979). A 130 K protein from chicken gizzard: its localization at the termini of microfilament bundles in cultured chicken cells. *Cell* **18**, 193-205.

Geiger, B., Dutton, A. H., Tokuyasu, K. T. and Singer, S. J. (1981). Immunoelectron microscope studies of membrane-microfilament interactions: distributions of alpha-actinin, tropomyosin, and vinculin in intestinal epithelial brush border and chicken gizzard smooth muscle cells. *J. Cell Biol.* **91**, 614-628.

Glukhova, M., Koteliansky, V., Sastre, X. and Thiery, J. P. (1995). Adhesion systems in normal breast and in invasive breast carcinoma. *Am. J. Pathol.* **146**, 706-716.

Gumbiner, B. M. (1996). Cell adhesion: the molecular basis of tissue architecture and morphogenesis. *Cell* **84**, 345-357.

Harborth, J., Elbashir, S. M., Bechert, K., Tuschl, T. and Weber, K. (2001). Identification of essential genes in cultured mammalian cells using small interfering RNAs. *J. Cell Sci.* **114**, 4557-4565.

Hazan, R. B., Kang, L., Roe, S., Borgen, P. I. and Rimm, D. L. (1997). Vinculin is associated with the E-cadherin adhesion complex. *J. Biol. Chem.* **272**, 32448-32453.

Humphries, J. D., Wang, P., Streuli, C., Geiger, B., Humphries, M. J. and Ballestrem, C. (2007). Vinculin controls focal adhesion formation by direct interactions with talin and actin. *J. Cell Biol.* **179**, 1043-1057.

Imamura, Y., Itoh, M., Maeno, Y., Tsukita, S. and Nagafuchi, A. (1999). Functional domains of alpha-catenin required for the strong state of cadherin-based cell adhesion. *J. Cell Biol.* **144**, 1311-1322.

Ireton, R. C., Davis, M. A., van Hengel, J., Mariner, D. J., Barnes, K., Thoreson, M. A., Anastasiadis, P. Z., Matrisian, L., Bundy, L. M., Sealy, L. et al. (2002). A novel role for p120 catenin in E-cadherin function. *J. Cell Biol.* **159**, 465-476.

Izard, T., Evans, G., Borgon, R. A., Rush, C. L., Bricogne, G. and Bois, P. R. (2004). Vinculin activation by talin through helical bundle conversion. *Nature* **427**, 171-175.

Izard, T., Tran Van Nhieu, G. and Bois, P. R. (2006). Shigella applies molecular mimicry to subvert vinculin and invade host cells. *J. Cell Biol.* **175**, 465-475.

Johnson, R. P. and Craig, S. W. (1995). F-actin binding site masked by the intramolecular association of vinculin head and tail domains. *Nature* **373**, 261-264.

Kawahara, E., Tokuda, R. and Nakanishi, I. (1999). Migratory phenotypes of HSC-3 squamous carcinoma cell line induced by EGF and PMA: relevance to migration of loosening of adhesion and vinculin-associated focal contacts with prominent filopodia. *Cell Biol. Int.* **23**, 163-174.

Kuroda, N., Naruse, K., Miyazaki, E., Hayashi, Y., Yoshikawa, C., Ashida, S., Moriki, T., Yamasaki, Y., Numoto, S., Yamamoto, Y. et al. (2000). Vinculin: its possible use as a marker of normal collecting ducts and renal neoplasms with collecting duct system phenotype. *Mod. Pathol.* **13**, 1109-1114.

Kuroda, N., Sugimoto, T., Ueda, S., Takahashi, T., Moriki, T., Sonobe, H., Miyazaki, E., Hayashi, Y., Toi, M., Hiroi, M. et al. (2001). Malignant phyllodes tumor of the breast with expression of osteonectin and vinculin. *Pathol. Int.* **51**, 277-282.

Lal, M., Song, X., Pluznick, J. L., Di Giovanni, V., Merrick, D. M., Rosenblum, N. D., Chauvet, V., Gottardi, C. J., Pei, Y. and Caplan, M. J. (2008). Polycystin-1 C-terminal tail associates with beta-catenin and inhibits canonical Wnt signaling. *Hum. Mol. Genet.* **17**, 3105-3117.

Lifschitz-Mercer, B., Czernobilsky, B., Feldberg, E. and Geiger, B. (1997). Expression of the adherens junction protein vinculin in human basal and squamous cell tumors: relationship to invasiveness and metastatic potential. *Hum. Pathol.* **28**, 1230-1236.

Maddugoda, M. P., Crampton, M. S., Shewan, A. M. and Yap, A. S. (2007). Myosin VI and vinculin cooperate during the morphogenesis of cadherin cell-cell contacts in mammalian epithelial cells. *J. Cell Biol.* **178**, 529-540.

Meyer, T. and Brinck, U. (1997). Immunohistochemical detection of vinculin in human rhabdomyosarcomas. *Gen. Diagn. Pathol.* **142**, 191-198.

Miranda, K. C., Khromykh, T., Christy, P., Le, T. L., Gottardi, C. J., Yap, A. S., Stow, J. L. and Teasdale, R. D. (2001). A dileucine motif targets E-cadherin to the basolateral cell surface in Madin-Darby canine kidney and LLC-PK1 epithelial cells. *J. Biol. Chem.* **276**, 22565-22572.

Moese, S., Selbach, M., Brinkmann, V., Karlas, A., Haimovich, B., Backert, S. and Meyer, T. F. (2007). The Helicobacter pylori CagA protein disrupts matrix adhesion of gastric epithelial cells by dephosphorylation of vinculin. *Cell Microbiol.* **9**, 1148-1161.

Noren, N. K., Niessen, C. M., Gumbiner, B. M. and Burridge, K. (2001). Cadherin engagement regulates Rho family GTPases. *J Biol. Chem.* **276**, 33305-33308.

Ory, D. S., Neugeboren, B. A. and Mulligan, R. C. (1996). A stable human-derived packaging cell line for production of high titer retrovirus/vesicular stomatitis virus G pseudotypes. *Proc. Natl. Acad. Sci. USA* **93**, 11400-11406.

Piedra, J., Martinez, D., Castano, J., Miravet, S., Dunach, M. and de Herreros, A. G. (2001). Regulation of beta-catenin structure and activity by tyrosine phosphorylation. *J. Biol. Chem.* **276**, 20436-20443.

Pokutta, S. and Weis, W. I. (2000). Structure of the dimerization and beta-catenin-binding region of alpha-catenin. *Mol. Cell* **5**, 533-543.

Raz, A., Zoller, M. and Ben, Z. e. (1986). Cell configuration and adhesive properties of metastasizing and non-metastasizing BSp73 rat adenocarcinoma cells. *Exp. Cell Res.* **162**, 127-141.

Sadano, H., Inoue, M. and Taniguchi, S. (1992). Differential expression of vinculin between weakly and highly metastatic B16-melanoma cell lines. *Jpn. J. Cancer Res.* **83**, 625-630.

Saunders, R. M., Holt, M. R., Jennings, L., Sutton, D. H., Barsukov, I. L., Bobkov, A., Liddington, R. C., Adamson, E. A., Dunn, G. A. and Critchley, D. R. (2006). Role of vinculin in regulating focal adhesion turnover. *Eur. J. Cell Biol.* **6**, 487-500.

Sheikh, F., Chen, Y., Liang, X., Hirschy, A., Stenbit, A. E., Gu, Y., Dalton, N. D., Yajima, T., Lu, Y., Knowlton, K. U. et al. (2006). alpha-E-catenin inactivation disrupts the cardiomyocyte adherens junction, resulting in cardiomyopathy and susceptibility to wall rupture. *Circulation* **114**, 1046-1055.

Somiari, R. I., Sullivan, A., Russell, S., Somiari, S., Hu, H., Jordan, R., George, A., Katenhusen, R., Buchowiecka, A., Arciero, C. et al. (2003). High-throughput proteomic analysis of human infiltrating ductal carcinoma of the breast. *Proteomics* **3**, 1863-1873.

Stemmer, V., de Craene, B., Berx, G. and Behrens, J. (2008). Snail promotes Wnt target gene expression and interacts with beta-catenin. *Oncogene* **27**, 5075-5080.

Subauste, M. C., Nalbant, P., Adamson, E. D. and Hahn, K. M. (2005). Vinculin controls PTEN protein level by maintaining the interaction of the adherens junction protein beta-catenin with the scaffolding protein MAGI-2. *J. Biol. Chem.* **280**, 5676-5681.

Takeichi, M. (1994). The cadherin cell adhesion receptor family: roles in multicellular organization and neurogenesis. *Prog. Clin. Biol. Res.* **390**, 145-153.

Tepass, U., Truong, K., Godt, D., Ikura, M. and Peifer, M. (2000). Cadherins in embryonic and neural morphogenesis. *Nat. Rev. Mol. Cell. Biol.* **1**, 91-100.

Verma, U. N., Surabhi, R. M., Schmaltieg, A., Becerra, C. and Gaynor, R. B. (2003). Small interfering RNAs directed against beta-catenin inhibit the in vitro and in vivo growth of colon cancer cells. *Clin. Cancer Res.* **9**, 1291-1300.

Watabe-Uchida, M., Uchida, N., Imamura, Y., Nagafuchi, A., Fujimoto, K., Uemura, T., Vermeulen, S., van Roy, F., Adamson, E. D. and Takeichi, M. (1998). alpha-Catenin-vinculin interaction functions to organize the apical junctional complex in epithelial cells. *J. Cell Biol.* **142**, 847-857.

Weiss, E. E., Kroemker, M., Rudiger, A. H., Jockusch, B. M. and Rudiger, M. (1998). Vinculin is part of the cadherin-catenin junctional complex: complex formation between alpha-catenin and vinculin. *J. Cell Biol.* **141**, 755-764.

Wheelock, M. J. and Johnson, K. R. (2003a). Cadherin-mediated cellular signaling. *Curr. Opin. Cell Biol.* **15**, 509-514.

Wheelock, M. J. and Johnson, K. R. (2003b). Cadherins as modulators of cellular phenotype. *Annu. Rev. Cell Dev. Biol.* **19**, 207-235.

Wiebe, J. P., Muzia, D., Hu, J., Szwajcer, D., Hill, S. A. and Seachrist, J. L. (2000). The 4-pregnene and 5alpha-pregnane progesterone metabolites formed in nontumorous and tumorous breast tissue have opposite effects on breast cell proliferation and adhesion. *Cancer Res.* **60**, 936-943.

Xiao, K., Allison, D. F., Buckley, K. M., Kottke, M. D., Vincent, P. A., Faundez, V. and Kowalczyk, A. P. (2003). Cellular levels of p120 catenin function as a set point for cadherin expression levels in microvascular endothelial cells. *J. Cell Biol.* **163**, 535-545.

Xu, W., Baribault, H. and Adamson, E. D. (1998a). Vinculin knockout results in heart and brain defects during embryonic development. *Development* **125**, 327-337.

Xu, W., Coll, J. L. and Adamson, E. D. (1998b). Rescue of the mutant phenotype by reexpression of full-length vinculin in null F9 cells; effects on cell locomotion by domain deleted vinculin. *J. Cell Sci.* **111**, 1535-1544.

Yamada, S., Pokutta, S., Drees, F., Weis, W. I. and Nelson, W. J. (2005). Deconstructing the cadherin-catenin-actin complex. *Cell* **123**, 889-901.

Yap, A. S., Crampton, M. S. and Hardin, J. (2007). Making and breaking contacts: the cellular biology of cadherin regulation. *Curr. Opin. Cell Biol.* **19**, 508-514.

Zemljic-Harpf, A. E., Ponrartana, S., Avalos, R. T., Jordan, M. C., Roos, K. P., Dalton, N. D., Phan, V. Q., Adamson, E. D. and Ross, R. S. (2004). Heterozygous inactivation of the vinculin gene predisposes to stress-induced cardiomyopathy. *Am. J. Pathol.* **165**, 1033-1044.

Zemljic-Harpf, A. E., Miller, J. C., Henderson, S. A., Wright, A. T., Manso, A. M., Elsherif, L., Dalton, N. D., Thor, A. K., Perkins, G. A., McCulloch, A. D. et al. (2007). Cardiac-myocyte-specific excision of the vinculin gene disrupts cellular junctions, causing sudden death or dilated cardiomyopathy. *Mol. Cell. Biol.* **27**, 7522-7537.

Ziegler, W. H., Liddington, R. C. and Critchley, D. R. (2006). The structure and regulation of vinculin. *Trends Cell Biol.* **16**, 453-460.

Journal of Cell Science